Available online at www.sciencedirect.com

SciVerse ScienceDirect

Advances in Space Research 52 (2013) 205–210

ADVANCES IN SPACE RESEARCH (a COSPAR publication)

www.elsevier.com/locate/asr

Generation mechanism of the whistler-mode waves in the plasma sheet prior to magnetic reconnection

X.H. Wei [a,*], J.B. Cao [b], G.C. Zhou [a], H.S. Fu [b], O. Santolík [c,d], H. Rème [e,f], I. Dandouras [e,f], N. Cornilleau [g], A. Fazakerley [h]

[a] State Key Laboratory of Space Weather, Center for Space Science and Applied Research, Chinese Academy of Sciences, Beijing, China
[b] Beihang University, Beijing 100190, China
[c] Institute of Atmospheric Physics of the Academy of Sciences of the Czech Republic, Charles University, Prague, Czech Republic
[d] Faculty of Mathematics and Physics, Charles University, Prague, Czech Republic
[e] IRAP, University of Toulouse, UPS-OMP, Toulouse, France
[f] CNRS, IRAP, 9 Ave. Colonel Roche, BP 44346, F-31028 Toulouse cedex 4, France
[g] CETP/UVSQ, Velizy, France
[h] Univ. College London, London, UK

Received 1 April 2012; received in revised form 16 February 2013; accepted 20 February 2013
Available online 5 March 2013

Abstract

The whistler-mode waves and electron temperature anisotropy play a key role prior to and during magnetic reconnection. On August 21, 2002, the Cluster spacecrafts encountered a quasi-collisionless magnetic reconnection event when they crossed the plasma sheet. Prior to the southward turning of magnetospheric magnetic field and high speed ion flow, the whistler-mode waves and positive electron temperature anisotropy are simultaneously observed. Theoretic analysis shows that the electrons with positive temperature anisotropy can excite the whistler-mode waves via cyclotron resonances. Using the data of particles and magnetic field, we estimated the whistler-mode wave growth rate and the ratio of whistler-mode growth rate to wave frequency. They are $0.0016f_{ce}$ (Electron cyclotron frequency) and $0.0086f_{ce}$, respectively. Therefore the whistler-mode waves can grow quickly in the current sheet. The combined observations of energetic electron beams and waves show that after the southward turning of magnetic field, energetic electrons in the reconnection process are accelerated by the whistler-mode waves.

Keywords: Whistler-mode waves; Electron temperature anisotropy; Reconnection; The plasma sheet

1. Introduction

The magnetic reconnection process is fundamentally important in understanding the solar wind–magnetosphere interactions. The magnetic reconnection is an efficient mechanism for the entry of the solar wind plasma to the Earth's magnetosphere and energy release in the magnetotail (Dungey, 1961; Vasyliunas, 1975). The magnetic reconnection process, the dynamics of the diffusion region is rather complex. Through magnetic reconnection, magnetic field energy is converted into plasma kinetic energy. Because of the importance in understanding eruptive macroscopic phenomena in magnetized plasmas, reconnection has been received increased attention.

Although the electron behavior is believed to be very important in the triggering of magnetic reconnection (Birn et al., 2001, 2005), a more in-depth understanding of the electron dynamics is still needed to explain the spontaneous onset of reconnection and to reveal how magnetic field energy is converted into kinetic energy in electron and ion fluids. Several mechanisms have been proposed to

* Corresponding author. Tel.: +86 01062613235.
E-mail address: xhwei@spaceweather.ac.cn (X.H. Wei).

0273-1177/$36.00 © 2013 COSPAR. Published by Elsevier Ltd. All rights reserved.
http://dx.doi.org/10.1016/j.asr.2013.02.016

explain the excitation of the whistler-mode waves. The most important one is the excitation mechanism by temperature anisotropies $A(v_r)$ and loss cones. The density of anisotropic electron component should be sufficiently low ($n(v_r) << n_0$), in order to not disturb the propagation of the whistler-mode waves (Kennel and Petschek, 1966; Etcheto et al., 1973). Electrons with positive temperature anisotropy can excite the whistler-mode waves through the gyro-resonance process (Kennel and Petschek, 1966; Etcheto et al., 1973; Fu et al., 2012), anomalous cyclotron resonance and Landau resonance. Using linearized Vlasov equation, Akimoto and Gray (1987) found that there exist obliquely propagating the whistler-mode waves instabilities in magnetotail, and these instabilities can be driven by electron beams, ion beams, and field-aligned currents. At scale of neither the ion inertial length nor the electron inertial length, the whistler-mode wave can grow. The peak of the maximum growth rate is found at the scale of ion Larmor radius (Cai et al., 2001).

The whistler-mode waves were observed in the magnetotail frequently. The quasi-parallel propagation of the observed the whistler-mode waves in the magnetotail plasma sheet suggests that the cyclotron resonance is the dominant process (Zhang et al., 1999; Gurnett et al., 1976; Scarf et al., 1974, 1984; Kennel et al., 1986; Farrell et al., 2002, 2003). Gurnett et al. (1976) suggested that the whistler-mode waves are most likely produced by current-driven plasma instabilities. It is suggested that the superthermal electrons with highly anisotropic pitch angle distributions can generate the whistler-mode waves. Zhang et al. (1999) analyzed the whistler-mode waves observed by Geotail in the magnetotail at radial distance ranging from $-210R_e$ to $-10R_e$, and found that the whistler-mode waves can exist in both plasma sheet and plasma sheet boundary layer, and propagate quasi-parallel to the ambient magnetic field with an average propagation angle of 23°. They thought that it is the energetic electron beams that generate the whistler-mode waves. The whistler-mode waves associated with reconnection in the Earth's magnetopause were also observed by Geotail (Deng and Matsumoto, 2001; Drake et al., 1997). Therefore the whistler-mode waves and magnetic reconnection are closely related to each other. Up to present, the satellite observations have shown that the whistler-mode waves exist in reconnection process and are most likely excited by electron beams generated by magnetic reconnection. However, the whistler-mode waves prior to reconnection are rarely reported. Wei et al. (2007) once reported that the burst of the whistler-mode waves appeared about 30 s earlier than the southward turning. They also found that the whistler-mode waves prior to the onset of magnetic reconnection are different from the waves in the whistler frequency range within magnetic reconnection.

Energetic electrons up to 300 keV were observed frequently during reconnection events by spacecrafts in magnetotail (Øieroset et al., 2002). The lower hybrid waves are also suggested to be responsible for the acceleration of energetic electrons (Cairns and McMillan, 2005). Recent Cluster observations (Imada et al., 2007) have provided some evidences for these acceleration mechanisms. The observations show the energetic electrons in the magnetic flux pile-up region close to the X-line and the observations can be explained the mechanism proposed by Hoshino et al. (2001). Some other reconnection observed by Cluster, however, indicates that the waves around lower hybrid frequency do not show a clear correlation with energetic electrons (Retino et al., 2008). The energetic electrons are directly accelerated by the electric field during unsteady reconnection (Retino et al., 2008; Asano et al., 2008; He et al., 2008). Magnetic islands may be an important agent responsible for the generation of energetic electrons (Chen et al., 2008; Retino et al., 2008; Oka et al., 2010; Wang et al., 2010).

In this paper we mainly focus on the relationship between the energetic electron and the whistler-mode waves prior to the onset of reconnection event. The results show that the electron temperature anisotropy can exist prior to the onset of reconnection event. The electrons can resonance with the whistler-mode waves. The paper is organized as follows. Section 2 gives a theoretical interpretation by using the whistler-mode wave instability. Section 3 summarizes the main conclusions.

2. The whistler-mode waves instability in current sheet prior to the reconnection onset

2.1. Overview the August 21, 2002 reconnection event and whistler-mode wave events

In this section we will simply review the reconnection event and the whistler-mode waves events on August 21, 2002. The reconnection and the whistler-mode wave event are discussed detail in the previous paper (Wei et al., 2007). The Cluster spacecrafts observed a reconnection event within the period 07:50UT – 08:00UT. The tailward high speed ion flow with southward magnetic field component is observed at 07:53:50 UT by C1 and C3, and at 07:54:05 UT by C4. The maximum velocity of tailward ion flow even exceeded 1500 km/s and the maximum southward magnetic field reached 20 nT. During reconnection event and before the magnetic field turned to southward, C1 and C2 at 07:53:18UT, are observed strong quasi-parallel propagating right-hand polarized whistler-mode waves. Similar features of waves for C3 are also found at 07:53:08UT.

2.2. The whistler-mode wave instability

The enhanced whistler-mode wave activities were observed simultaneously in the current sheet by C1, C2 and C3 before the reconnection event observed. Electrons with a positive temperature anisotropy $A(v_r)$ can excite the whistler-mode waves by cyclotron resonances (Kennel and Petschek, 1966; Etcheto et al., 1973; Fu et al., in press

a,b, 2011b). The resonance condition between the whistler-mode waves and non-relativistic electrons can be described as (Fu et al., 2011a) $f - f_{ce} = v_{//}k_{//}$. The density of hot electron component should be sufficiently low ($n(v_r) << n_0$), in order not to disturb the propagation of the whistler mode waves. The whistler-mode wave instability can arise due to the free energy stored in positive temperature anisotropy of hot electron component. The dispersive relation for the whistler-mode wave propagation parallel to the magnetic field is

$$\left(\frac{ck_{\|}}{f}\right)^2 \approx \frac{(f_{pe})^2}{f(f_{ce}-f)} \tag{1}$$

The electron resonant velocity v_r is defined by the cyclotron resonance condition as

$$v_r = (f - f_{ce})/k_{\|} \tag{2}$$

Using the dispersion relation (1) and the resonance condition (2), the parallel energy of resonant electrons can be written

$$E_r = \frac{1}{2}\left(mv_r^2\right) = E_c\frac{f_{ce}}{f}\left(1-\frac{f}{f_{ce}}\right)^3 \tag{3}$$

where $E_c = B^2/8\pi n_0$ is a characteristic energy for cyclotron interactions. The growth rate for the whistler-mode wave instability is (Kennel and Petschek, 1966; Etcheto et al., 1973; Fu et al., in press a)

$$\gamma = \pi f_{ce}\left(1-\frac{f}{f_{ce}}\right)^2 n(v_r)[A(v_r) - A_c] \tag{4}$$

where $n(v_r)$ is density that may be roughly interpreted as the fraction of the total electron distribution in a range $\Delta v_{//} = (f_{ce} - f)/k_{//} = v_r$ about cyclotron anisotropy, $A(v_r)$, A_c represent temperature anisotropy of resonant electrons, and critical temperature anisotropy defined, respectively, by

$$n(v_r) = 2\pi\frac{f_{ce}-f}{k}\int_0^{\infty} v_{\perp}Fdv_{\perp}\Big|_{v_{\|}=v_r} \tag{5}$$

$$A(v_r) = \frac{\int_0^{\infty}\left(v_{//}\frac{\partial F}{\partial v_{\perp}} - v_{\perp}\frac{\partial F}{\partial v_{//}}\right)\frac{v_{\perp}^2}{v_{//}}dv_{\perp}}{2\int_0^{\infty} v_{\perp}Fdv_{\perp}}\Bigg|_{v_{//}=v_r} = \frac{\int_0^{\infty} v_{\perp}\tan\alpha\frac{\partial F}{\partial \alpha}dv_{\perp}}{2\int_0^{\infty} v_{\perp}Fdv_{\perp}}\Bigg|_{v_{//}=v_r} \tag{6}$$

$$A_c = \frac{1}{f_{ce}/f - 1} \tag{7}$$

where f_{ce} is the electron cyclotron frequency, $k_{//}$ the parallel wave number, v_r the resonant velocity, f the wave frequency, F the total electron distribution function, $v_{//}$ the electron parallel velocity, $v_{\perp}$ the electron perpendicular velocity, and $\alpha = \tan^{-1}(-v_{\perp}/v_{//})$ is pitch angle. The resonant electrons must have a specific parallel velocity so as to resonate with a wave of frequency f. But they may have any perpendicular velocity. In fact the stability criterion involves the properties of the distribution function integrated over all perpendicular velocities. $A(v_r)$ is a measure of pitch angle anisotropy. Since $n(v_r)$ is always positive, waves are unstable when $A(v_r) > A_e$. A sufficient condition for instability for waves resonant with electrons is simply that $\partial F/\partial\alpha$ be positive everywhere. Therefore, any mechanism that flattens the pitch angle of every particle, such as magnetic field compression, makes the tail of the electron distribution (where $E_r > B^2/8\pi N$) unstable to noise emission in the whistler mode. Whether or not a whistler mode wave emission is unstable depends only on the electron pitch angle anisotropy $A(v_r)$. Rudolf and Wolfgang (1997) qualitatively discussed the relationship among growth rate, the whistler-mode wave frequency and $A(v_r)$. Their analysis shows that the whistler-mode waves instability can be excited when the temperature anisotropy $A(v_r)$ is near 0.02.

2.3. The growth rate for whistler-mode wave instability

The data used in this study are from the Cluster spacecrafts. Electron data from PEACE instrument (Johnstone et al., 1997). The PEACE instrument has two sensor heads, a low-energy electron analyzer (LEEA) and a high-energy electron analyzer (HEEA), which are mounted on opposite sides of the spacecrafts. In this study, we use the pitch angle distribution data from PEACE–LEEA. Fig. 1 shows the Phase Space Density from the PEACE instrument low-energe sensor (LEEA) at 07:53:14UT. The electron distribution function is anisotropic at certain energy.

Fig. 2 shows the dimensionless growth rate, the resonance energy, temperature anisotropy and $n(v_r)$ calculated by using Eqs. (4)–(7) and the data (PEACE–LEEA) observed by C3 at 07:53:14UT. The growth rate is positive in the frequency range 0.138–0.33f_e (see the panel a). The maximal growth rate is 0.0016 at the frequency 0.186. The horizontal axis shows the frequency and dimensionless frequency. The first panel shows the dimensionless growth rate, and the maximal growth rate is at the frequency of 105 Hz (see the panel a). The corresponding electron resonance energy in panel b is 0.15 keV. The third panel shows the temperature anisotropy (solid line) $A(v_r)$, $A(v_r)$–A_e (dashed line), and A_e (dash dot line). The corresponding temperature anisotropy (solid line in the third panel) showed by panel fourth is 1.35. During the whole frequency range, the $n(v_r)$ is very low (see the panel d). The $n(v_r)$ satisfies the low density condition $n(v_r) << n_0$.

Table 1 lists the results calculated by using Eqs. (4)–(7) and Cluster data. The second row shows the time at which the data recorded by spacecrafts. The third row shows maximal the whistler-mode wave growth rate. The fourth, fifth, sixth and seventh rows show the electron resonance energy, the temperature anisotropy the whistler wave resonance frequency and the whistler wave resonance dimensionless frequency corresponding to the maximal growth rate, respectively. The above calculation results show that there are positive growth rate in the current sheet prior

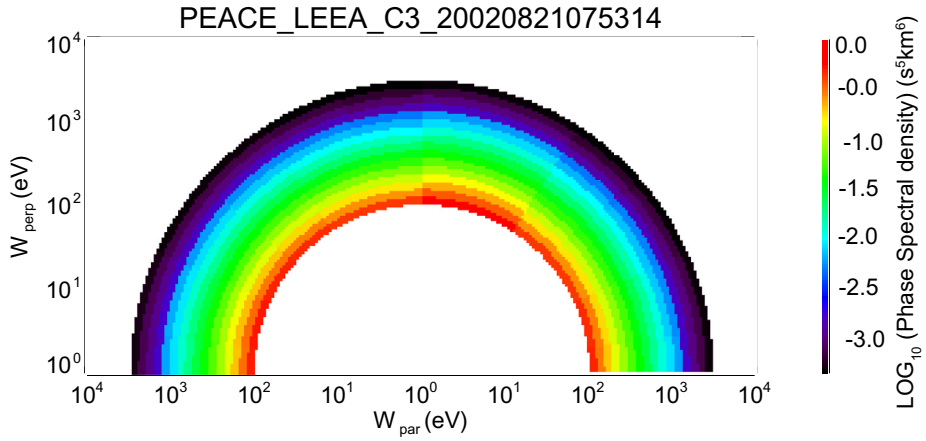

Fig. 1. Electron distribution functions measured by LEEA/PEACE. The phase space density is plotted in color according to the right color bar.

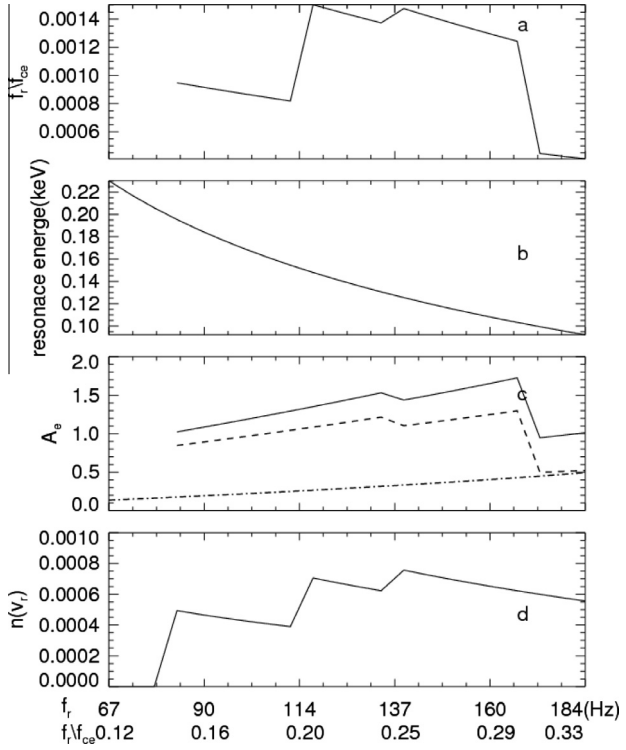

Fig. 2. The growth rate (a), electron resonance energy (b), A_e (c) and the $n(v_r)$ (d) as a function of wave frequency.

to magnetic reconnection. The maximal growth rate is obtained by using the data from the C3. The corresponding the whistler wave resonance frequency are the lowest, and the temperature anisotropy is higher than those obtained at C4.

The maximal growth rate of whistler-mode wave frequencies measured by C1, C2, and C4 are all lower than the resonance frequency (Wei et al., 2007). The whistler-mode waves observed by C1, C2, and C4 cannot be excited easily by the temperature anisotropy electron. The whistler-mode wave frequency detected by C3 is very close to resonance frequency. The whistler-mode waves observed by C3 can be excited easily by the temperature anisotropy electron.

3. Discussion and Conclusion

The electron temperature anisotropy A_e observed by C3 at 07:53:10UT and 07:53:14UT is 1.35. The maximal growth rate is 0.00077 and 0.0016, respectively. The whistler-mode wave activities become strong at 07:53:08UT. The electron temperature time resolution is 4 s. The whistler wave frequency is about 100 Hz during 07:53:08–07:53:12UT. The resonance electron energy is about 100 eV. The resonance wave frequency is about 100 Hz. The resonance wave frequency is very close to the whistler-mode wave frequency observed by spacecrafts. The above results show that the whistler-mode wave can be enhanced in the current sheet before magnetic reconnection. At 07:53:10UT, the resonance electron velocity is anti-parallel to magnetic field and at 07:53:14UT the resonance electron velocity is parallel to magnetic field. The opposite propagating whistler-mode waves and electrons can generate cyclotron resonance. The antiparallel and parallel resonance electron observed at same satellite show the whistler-mode wave direction turned at different time. The resonance wave frequency calculated by C1, C2, C4 data and Eq. (1) is higher than the whistler-mode wave frequency observed by C1, C2, C4. The electron and the wave cannot resonate easily. At 07:53:00UT, C1 was approximately located at (−18.36, −4.27, 0.22) R_e, C2 at (−18.74, −4.02, 0.39) R_e, C3 at (−18.81, −4.30, −0.04) R_e and C4 at (−19.0, −4.40, 0.59) R_e. The total magnetic field observed by C3 is the smallest. The whistler-mode waves are observed by C1 and C2 at the same time. The whistler wave and electron anisotropy observed by C3 are earlier than that observed by C1 and C2. According to the Cluster station and the above analysis, C3 are very near to the electron current sheet center. C1 and C2 may be at the edge of electron current sheet. Both the theory and observations show the whistler can be excited. After the high speed tailward flow was observed by C1, C2 and

Table 1
Characteristics of waves, temperature anisotropy and resonant energy.The results are derived from Eqs. (4)–(7) and the Cluster data. The second row shows the time at which the data is recorded by spacecrafts. The third row shows the maximal growth rate. The fourth row shows the resonance energy at the maximal growth rate. The fifth row shows the temperature anisotropy at the maximal growth rate. The sixth row shows the resonance wave frequency at the maximal growth rate.

Satellite	C1	C2	C3	C4
Time (UT)	07:53:21	07:53:18	07:53:14	07:53:25
Max growth rate	0.0012	0.0009	0.0016	0.00053
Resonance energy (keV)	0.35	0.14	0.155	0.25
Temperature anisotropy	1.5	1.4	1.35	0.6
Resonance frequency (Hz)	163	267	105	173
Dimensionless frequency $\left(\frac{f}{f_{ce}}\right)$	0.2	0.33	0.187	0.285

C3, the whistler-mode waves become stronger, and the relationship between the whistler-mode waves and the high speed tailward flow becomes very complicated. The calculation results also show the electron and whistler-mode wave can resonate after the reconnection. The appearances of southward magnetic field observed by C1, C2 and C3 are later than the high speed tailward flow. A high speed tailward ion flow and a large southward magnetic field component synchronously observed by spacecrafts generally can be produced by magnetic reconnection. The magnetic reconnection event observed by spacecrafts is later than the whistler-mode waves. The whistler-mode wave activities are observed before and after the southward turning of B_z component. However their characteristics of waves are obviously different (Wei et al., 2007). The observations of electrons also show that during the reconnection process, there are many bursts of energetic electrons (Wei et al., 2007).

The relationship between whistler-mode waves and reconnection is very complicated. Up to present, the problem of triggering of magnetic reconnection in the tail is still not fully understood. The whistler-mode wave activities observed by satellites in the current sheet prior to the onset of reconnection will help to shed light on this problem. During the reconnection event, the whistler-mode wave activities became stronger. During the period where the electron temperature anisotropy is bigger than 1.35, the whistler-mode waves activities were observed by Cluster satellites. The theoretical whistler-mode wave growth rate calculated based on the data of observed magnetic field and plasma is about $0.0016\omega_{ge}$. The ratio of whistler-mode wave growth rate to wave frequency is about 0.0086. Therefore, whistler-mode waves can grow quickly in the current sheet. The small discrepancy between theoretic and observational values of wave frequency is possibly caused by several simple assumptions adopted in the calculation of dispersion equation of whistler-mode wave. Electrons with positive temperature anisotropy can excite whistler-mode mode waves by cyclotron resonances. The quasi-parallel propagation of the observed whistler-mode waves suggests that the cyclotron resonance is the dominant process. The whistler-mode waves have a short time to grow. Furthermore, not all electron beams possess positive temperature anisotropy. Electron beams with negative temperature anisotropy cannot excite the whistler-mode waves. It can only excite the firehose instability. This may be the reason why the whistler-mode waves are observed discontinuously. After the onset of magnetic reconnection, the whistler-mode waves are stronger than before. The whistler-mode waves associated with the magnetic reconnection event is different from the whistler-mode waves in the current sheet. In this paper the generation mechanism of the whistler wave in the current sheet is discussed. The results presented in this work reveal the status of plasma sheet prior to magnetic reconnection and may provide an important hint of how magnetic reconnection is triggered.

Acknowledgements

This work was supported by NSFC grant 40804045 and 41174144 and the Spacialized Research Fund for State Key Laboratories of China. We greatly acknowledge the CLUSTER data on CAA webset.

References

Akimoto, K., Gray, S.P. Electro/ion whistler instabilities and magnetic noise bursts. J. Geophys. Res. 92 (A10), 11209–11214, 1987.

Asano, Y. et al. Electron flat-top distributions around the magnetic reconnection region. J. Geophys. Res. 113, A01207, http://dx.doi.org/10.1029/2007JA012461, 2008.

Birn, J. et al. Geospace environmental modeling (GEM) magnetic reconnection challenge. J. Geophys. Res. 106, 3715, 2001.

Birn, J. et al. Forced magnetic reconnection. Geophys. Res. Lett. 32, L06105, http://dx.doi.org/10.1029/2004GL022058, 2005.

Cai, C.L., Cao, J.B., Zhou, G.C., Wang, D.J. Whistler turbulence at the magnetopause: a nonlinear generation mechanism. Phys. Plasmas 8 (1), 272–276, 2001.

Cairns, I.H., McMillan, B.F. Electron acceleration by lower hybrid waves in magnetic reconnection regions. Phys. Plasmas 12, 102110, http://dx.doi.org/10.1063/1.2080567, 2005.

Chen, L.-J. et al. Observation of energetic electrons within magnetic islands. Nat. Phys. 4, 19–23, http://dx.doi.org/10.1038/nphys777, 2008.

Deng, X.H., Matsumoto, H. Rapid magnetic reconnection in the Earth's magnetosphere mediated by whistler waves. Nature 410, 557–560, 2001.

Dungey, J.W. Interplanetary field and the auroral zones. Phys. Res. Lett. 6, 47–48, 1961.

Drake, J.F., Biskamp, D., Zeiler, A. Breakup of the electron current layer during 3-D collisionless magnetic reconnection. Geophys. Res. Lett. 24, 2921–2924, 1997.

Etcheto, J., Gexdrin, R., Sokomon, J., Roux, A. A self-consistent theory of magentospheric ELF hiss. J. Geophys. Res. 78, 8150, 1973.

Farrell, W.M., Desch, M.D., Kaiser, M.L., Goetz, K. The dominance of electron plasma waves near a reconnection X-line. Geophys. Res. Lett. 29 (19), 1902, http://dx.doi.org/10.1029/2002GL014662, 2002.

Farrell, W.M., Desch, M.D., Ogilvie, K.W., Kaiser, M.L., Goetz, K. The role of upper hybrid waves in magnetic reconnection. Geophys. Res. Lett. 30 (24), 2259, http://dx.doi.org/10.1029/2003GL01549, 2003.

Fu, H.S., Cao, J.B., Mozer, F.S., Lu, H.Y., Yang, B., (in press a), Chorus intensification in response to interplanetary shock: THEMIS observations, J. Geophys. Res.

Fu, H.S., Cao, J.B., Zong, Q.-G., Lu, H.Y., Huang, S.Y., Wei, X.H., Ma, Y.D., (in press b), The role of electrons during chorus intensification: energy source and energy loss, J. Atmos. Terr. Phys.

Fu, H.S., Cao, J.B., Yang, B., Lu, H.Y. Electron loss and acceleration during storm time: the contribution of wave-particle interaction, radial diffusion, and transport processes. J. Geophys. Res. 116, A10210, http://dx.doi.org/10.1029/2011JA016672, 2011a.

Fu, H.S., Khotyaintsev, Y.V., André, M., Vaivads, A. Fermi and betatron acceleration of suprathermal electrons behind dipolarization fronts. Geophys. Res. Lett. 38, L16104, http://dx.doi.org/10.1029/2011GL048528, 2011b.

Gurnett, D.H., Frank, L.A., Lepping, R.P. Plasma waves in the distant magnetotail. J. Geophys. Res. 81 (34), 6059–6071, 1976.

Hoshino, M., Mukai, T., Terasawa, T., Shinohara, I. Suprathermal electron acceleration in magnetic reconnection. J. Geophys. Res. 106 (25), 997, 979-25, 2001.

Imada, S., Nakamura, R., Daly, P.W., Hoshino, M., Baumjohann, W., Mühlbachler, S., Balogh, A., Re'me, H. Energetic electron acceleration in the downstream reconnection outflow region. J. Geophys. Res. 112, A03202, http://dx.doi.org/10.1029/2006JA011847, 2007.

Johnstone, A.D. et al. PEACE: a plasma electron and current experiment. Space Sci. Rev. 79, 351–398, 1997.

Kennel, C.F., Coroniti, F.V., Scarf, F.L. Plasma waves in the magnetotail flux ropes. J. Geophys. Res. 91, 1424, 1986.

Kennel, C.F., Petschek, H.E. Limit on stably trapped particle fluxes. J. Geophys. Res. 71, 1, 1966.

Oka, M., Fujimoto, M., Shinohara, I., Phan, T.D. "Island surfing" mechanism of electron acceleration during magnetic reconnection. J. Geophys. Res. 115, A08223, http://dx.doi.org/10.1029/2010JA015392, 2010.

Øieroset, M., Lin, R.P., Phan, T.D., Larson, D.E., Bale, S.D. Evidence for electron acceleration up to 300 keV in the magnetic reconnection diffusion region of earth's magnetotail. Phys. Rev. Lett. 89 (19), http://dx.doi.org/10.1103/PhysRevlett.89195001, 2002.

Retino', A. Cluster observations of energetic electrons and electromagnetic fields within a reconnecting thin current sheet in the Earth's magnetotail. J. Geophys. Res. 113, A12215, http://dx.doi.org/10.1029/2008JA013511, 2008.

Rudolf, Treumann, A., Wolfgang, Baumjohann Electromagnetic instabilities, in: Advanced Space Plasma Physics. Imperial College Press, London, UK, pp. 105–114, 1997.

Scarf, F.L., Cornoniti, F.V., Kennel, C.F., Fredricks, R.W., Curnett, D.A., Smisth, E.J. ISEE 3 wave measurements in the distant geomagnetic tail and boundary layer. Geophys. Res. Lett. 11, 335–339, 1984.

Scarf, F., Frank, K., Ackerson, R., Lepping Plasma wave turbulence at distant crossings of the plasma sheet boundaries and neutral sheet. Geophys. Res. Lett. 1, 189, 1974.

Vasyliunas, V.M. Theoretical models of magnetic field line merging. Rev. Geophys. 13, 303–336, 1975.

Wei, X.H., Cao, J.B., Zhou, G.C., Santolík, O., Re'me, H., Dandouras, I., Cornilleau-Wehrlin, N., Lucek, E., Carr, C.M., Fazakerley, A. J. Geophys. Res. 112, A10225, http://dx.doi.org/10.1029/2006JA01177, 2007.

Wang, R., Lu, Q., Huang, C., Wang, S. Multispacecrafts observation of electron pitch angle distributions in magnetotail reconnection. J. Geophys. Res. 115, A01209, http://dx.doi.org/10.1029/2009JA014553, 2010.

Zhang, Y., Matsumoto, H., Kojima, H. Whistler mode waves in the magnetotail. J. Geophys. Res. 104 (A12), 28633–28644, 1999.